

Poisoning by air of AB₅ type rare-earth nickel hydrogen-absorbing alloys

T. Imoto, K. Satoh, K. Nishimura, T. Yonesaki, S. Fujitani, I. Yonezu

SANYO Electric Co Ltd, New Materials Research Center, 1-18-13 Hashiridani, Hirakata City, Osaka 573, Japan

Received 19 September 1994

Abstract

Poisoning by air of $\text{Mm}_{0.9}\text{Y}_{0.1}\text{Ni}_{4.9}\text{Mn}_{0.1}$ and $\text{LaNi}_{4.55}\text{Al}_{0.45}$ alloys with CaCu_5 structure was studied to clarify their applicability to refrigeration systems. The decrease in hydrogen capacity on hydrogen absorption–desorption cycling with air contamination was limited to a certain degree under an extended air concentration up to 1.0 vol.%. The poisoned alloys recovered their hydrogen-absorbing capacity on reactivation treatment. These results and X-ray powder diffraction analysis suggest that the degradation was not caused by complete oxidation. Thus, we propose that the degradation is caused by adsorption of oxygen in air, and that the poisoned state is an intermediate state which is more stable than the adsorption equilibrium state but less stable than the oxidation state. Poisoning by adsorption was analyzed using Langmuir's adsorption theory to explain the relations between the degradation rate and concentration of air.

Keywords: Hydrogen; Poisoning behaviour; Refrigeration system; Adsorption

1. Introduction

In recent years, global environmental problems such as global warming caused by carbon dioxide and destruction of the ozone layer by chlorofluorocarbons, are gathering widespread attention. We have been developing heat utilization systems such as heat storage, heat transportation systems and an F-class refrigeration system using hydrogen-absorbing alloys [1–3].

In particular, the refrigeration system is of great importance because it is free from chlorofluorocarbons, and can be driven by thermal energy including solar or industrial waste heat. This refrigeration system consists of two types of hydrogen-absorbing alloy with different equilibrium hydrogen pressures, a high-pressure alloy M₁ and a low-pressure alloy M₂ [4]. The refrigeration heat of around 253 K is generated by the endothermic reaction of hydrogen desorption from alloy M₁, while the desorbed hydrogen is absorbed into alloy M₂ at ambient temperature. The reverse reaction of hydrogen transfer from alloy M₂ to alloy M₁ occurs on heating alloy M₂ to around 423 K utilizing solar or industrial waste heat.

In the refrigeration heat generation process, the hydrogen pressure is usually below atmospheric pressure, which can cause the alloys to be poisoned by air

invading the alloy vessel. Therefore, the characterization of poisoning by air of the alloys is important for ensuring reliability of the refrigeration system.

The influences of O₂, N₂ and CO on the characteristics of hydrogen-absorbing alloys have already been studied [5–9], but the influence of air has not been studied quantitatively. In this work, the poisoning effect of air on hydrogen-absorbing alloys with CaCu_5 structure was studied to examine their applicability to refrigeration systems. $\text{Mm}_{0.9}\text{Y}_{0.1}\text{Ni}_{4.9}\text{Mn}_{0.1}$ and $\text{LaNi}_{4.55}\text{Al}_{0.45}$ alloys, which were developed as alloy M₁ and alloy M₂ respectively in the F-class refrigeration system, were employed for testing of the performance on cycling using hydrogen gas containing up to 1.0 vol.% air.

2. Experimental procedure

Sample alloys with compositions $\text{Mm}_{0.9}\text{Y}_{0.1}\text{Ni}_{4.9}\text{Mn}_{0.1}$ and $\text{LaNi}_{4.55}\text{Al}_{0.45}$ were prepared by induction melting the mixture of Mm and raw metals with 99.9% purity and annealing for 86.4 ks at 1273 K in vacuum. The alloys obtained were crushed and ground into powder of about 250 μm size.

These samples were used to examine the performance on hydrogen absorption–desorption cycling for up to

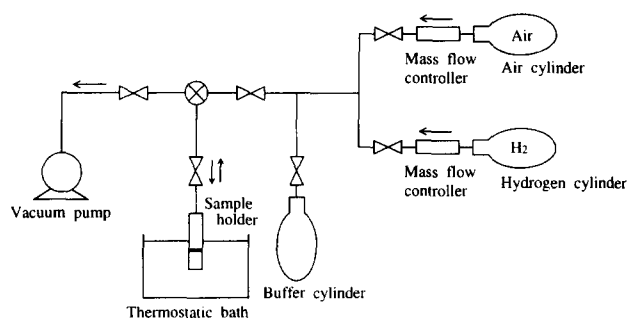


Fig. 1. Experimental apparatus.

200 cycles with air-containing hydrogen gas using the apparatus shown in Fig. 1. The hydrogen absorption-desorption cycling was carried out by pressurizing and evacuating between 1.5 MPa and 0.1 Pa at 313 K. The air concentration in hydrogen was regulated between 0.0 vol.% and 1.0 vol.%. P - C isotherms of the samples after the initial activation and after 200 cycles with air-containing hydrogen gas were measured with pure hydrogen gas with a Sieverts apparatus. The initial activation treatment was conducted by repeating pure hydrogen gas pressurization at 1 MPa and evacuation for 3.6 ks at 363 K. The zero-point of hydrogen content was set by evacuation with a rotary pump at the measured temperature of 363 K. The maximum hydrogen capacity of the alloys was analyzed using a thermodynamic model of P - C isotherms [10].

The crystal structure was determined using X-ray powder diffractometry with Cu $K\alpha$ radiation. The powder samples were coated with epoxy resin to prevent oxidation during the measurement process.

3. Results

3.1. Relation between the degradation behavior and air concentration

The hydrogen-absorbing capacity of both $\text{Mm}_{0.9}\text{Y}_{0.1}\text{Ni}_{4.9}\text{Mn}_{0.1}$ and $\text{LaNi}_{4.55}\text{Al}_{0.45}$ alloys decreased linearly with the number of cycles at all air concentrations. The degradation at 0.0 vol.% is intrinsic, 2.2% in the $\text{Mm}_{0.9}\text{Y}_{0.1}\text{Ni}_{4.9}\text{Mn}_{0.1}$ alloy and 0.9% in the $\text{LaNi}_{4.55}\text{Al}_{0.45}$ alloy. The degradation rates were affected greatly by the air concentration. Fig. 2 shows the absorption P - C isotherm at 313 K after 200 cycles for air concentrations between 0.0 vol.% and 1.0 vol.%.

The maximum hydrogen capacity determined using the P - C isotherm model [10] decreased from 1.46 mass% to 1.21 mass% in the $\text{Mm}_{0.9}\text{Y}_{0.1}\text{Ni}_{4.9}\text{Mn}_{0.1}$ alloy and from 1.33 mass% to 1.19 mass% in the $\text{LaNi}_{4.55}\text{Al}_{0.45}$ alloy with increasing the air concentration from 0.0 vol.% to 1.0 vol.%. The decrease in capacity saturated in both alloys. The plateau slope and pressure levels were not affected by the air concentration.

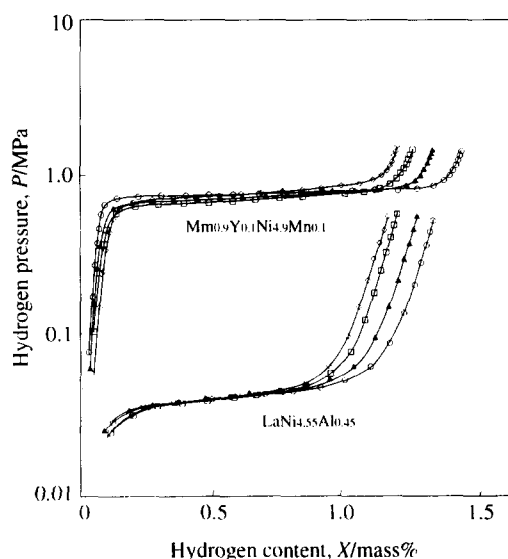


Fig. 2. Hydrogen-absorbing P - C isotherms at 313 K after 200 cycles with air-containing hydrogen gas: \circ 0.0 vol.% air, \blacktriangle 0.1 vol.% air, \square 0.3 vol.% air, \diamond 1.0 vol.% air.

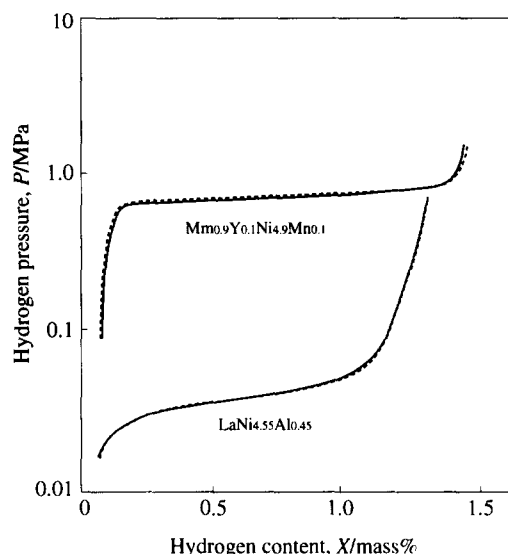


Fig. 3. Hydrogen-absorbing P - C isotherms at 313 K after exposing the alloys to hydrogen gas containing 0.3 vol.% air: --- after initial activation, — after exposure for 604.8 ks.

3.2. Exposure experiment

The influence of static storage on the degradation behavior under air-containing hydrogen gas was examined. The initially activated samples were exposed to hydrogen gas of 1 MPa containing 0.3 vol.% air for 604.8 ks, which corresponds to the length of a hydrogen absorption-desorption test of 200 cycles.

The result is shown in Fig. 3. No difference between P - C isotherms of the initially activated samples and exposure-tested samples was observed in either alloy. This result indicates that degradation occurs by a hy-

drogen absorption–desorption process, not by static storage.

3.3. Reactivation treatment

The reactivating behavior of the poisoned alloys was examined. It is known that heat treatment of a damaged alloy is effective for recovering the hydrogen-absorbing capacity [9]. In this work, reactivation treatment was performed by evacuating the samples which were poisoned by 0.3 vol.% air over 200 cycles with a rotary pump at an elevated temperature of 363 K for 18 ks and thereafter by pressurizing at 1.8 MPa pure hydrogen gas. After the reactivation treatment, the hydrogen capacities were measured using pure hydrogen gas.

The results are shown in Fig. 4. The hydrogen capacity recovery ratio of $\text{Mm}_{0.9}\text{Y}_{0.1}\text{Ni}_{4.9}\text{Mn}_{0.1}$ alloy was about 50% of the lost capacity, excluding the intrinsic capacity, and that of $\text{LaNi}_{4.55}\text{Al}_{0.45}$ alloy was about 60%.

It is reported that N_2 gas does not contribute to the degradation of LaNi_5 [9]. Accordingly, we consider that the degradation is caused mainly by oxygen. Furthermore, the reactivation temperature of 363 K is much lower than the reduction point of metal oxides. Therefore, the degradation and recovery of the hydrogen capacity are considered not to be caused by oxidation and reduction of the component metals.

3.4. X-ray powder diffraction

Analysis of the crystal structure was conducted by X-ray powder diffractometry on the tested samples with 0.0 vol.% and 0.3 vol.% air. The results for the $\text{LaNi}_{4.55}\text{Al}_{0.45}$ alloy are shown in Fig. 5. X-ray diffraction patterns of both samples showed broadening of the

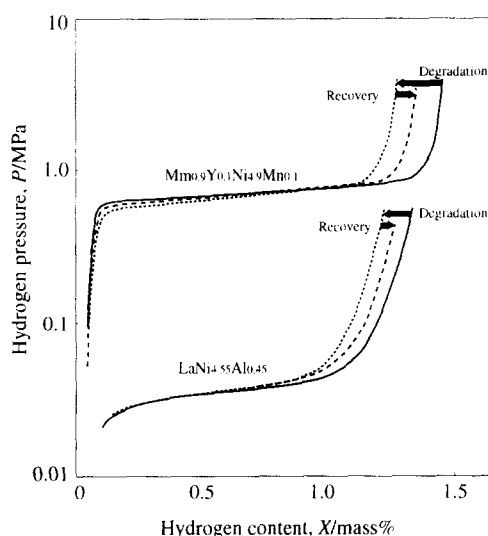


Fig. 4. Reactivation behavior of the alloys poisoned by air after 200 cycles: — 0.0 vol.% air, ···· 0.3 vol.% air, --- after reactivation treatment.

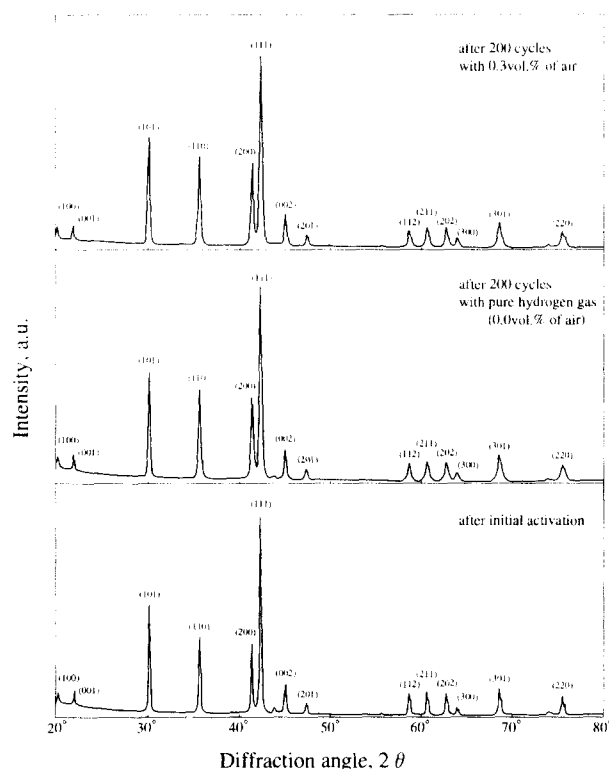


Fig. 5. X-ray powder diffraction patterns of the $\text{LaNi}_{4.55}\text{Al}_{0.45}$ alloy after 200 cycles.

peaks as is usually observed [11], but all of the peaks were assigned to the CaCu_5 structure and oxide peaks were not observed even in the poisoned samples.

4. Discussion

From the results of the cycling and exposure tests, the state of static storage at adsorption equilibrium is not the poisoned state. However, from the results of the reactivation treatment and X-ray powder diffraction analysis, the degradation is not caused by complete oxidation and therefore the state of oxidation is not the poisoned state.

Consequently, we propose that the degradation is caused by adsorption of oxygen in air at the surface of the alloys, and the adsorption state changes into the poisoned state every hydrogen absorption–desorption cycle, at a rate which is proportional to the surface concentration of air adsorbed. In other words, as shown in Fig. 6, the poisoned state (B) is an intermediate state, which is more stable than the adsorption equilibrium state (A) but less stable than the oxidation state (C).

Degradation models have already been studied quantitatively [12,13]. However, from calculations using conventional models, the degradation ratio reaches 100% with increasing air concentration. In this work, the degradation ratio was limited to 20% at most. Therefore,

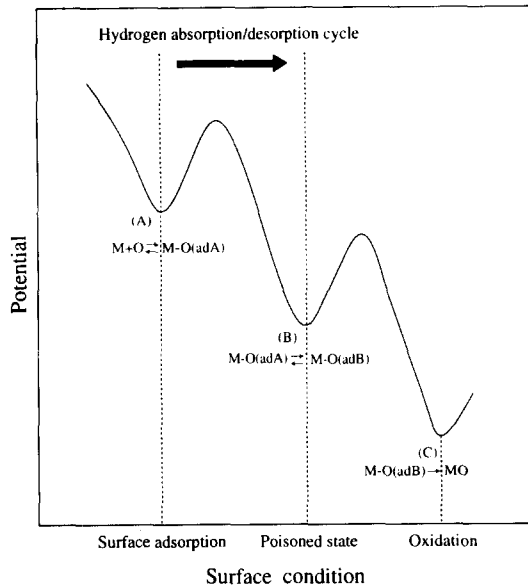


Fig. 6. An air poisoning model for the hydrogen-absorbing alloys.

the conventional models do not seem able to give a rational explanation for our experimental results.

Accordingly, a new degradation model was examined by applying a Langmuir-type adsorption isotherm to the poisoned state.

The degradation ratio R on cycling with air-containing hydrogen gas is the sum of the intrinsic degradation R_{in} and extrinsic degradation R_{ex} by poisoning as given in Eq. (1):

$$R = R_{in} + R_{ex} \quad (1)$$

Using an intrinsic degradation ratio r_{in} per cycle, R_{in} is given as

$$R_{in} = Nr_{in} \quad (2)$$

where N is the number of cycles.

If the adsorption equilibrium (A) is changed to the poisoned state (B) with a rate constant k for each cycle and, therefore, the extrinsic degradation R_{ex} is proportional to the surface coverage θ of the adsorption element and cycle number N , the degradation ratio R_{ex} can be written as

$$R_{ex} = Nk\theta \quad (3)$$

Then a Langmuir-type adsorption isotherm in Eq. (4) is applied to this model:

$$\theta = \frac{bc}{1+bc} \quad (4)$$

where b is an adsorption equilibrium constant and c is the air concentration. This leads from Eq. (3) to Eq. (5):

$$R_{ex} = Nk \frac{bc}{1+bc} \quad (5)$$

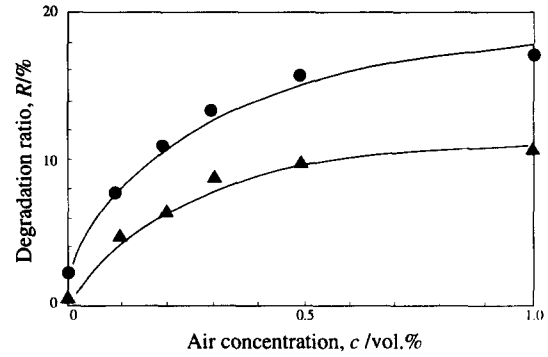


Fig. 7. Agreement of the experimental data with the proposed degradation model using the Langmuir-type adsorption isotherm: ● measured point of $Mm_{0.9}Y_{0.1}Ni_{4.9}Mn_{0.1}$, ▲ measured point of $LaNi_{4.55}Al_{0.45}$, — fitted lines.

Table 1
Parameters in the proposed degradation model

Alloy	k (10^{-4} cycle $^{-1}$)	b (vol.% $^{-1}$)	r_{in} (10^{-4} cycle $^{-1}$)
$Mm_{0.9}Y_{0.1}Ni_{4.9}Mn_{0.1}$	9.52	3.86	1.10
$LaNi_{4.55}Al_{0.45}$	5.59	5.60	0.45

Consequently, the degradation ratio R is formulated as

$$R = Nr_{in} + Nk \frac{bc}{1+bc} \quad (6)$$

Using this model, relations between the degradation ratio R and the air concentration c were analyzed. The fitted lines were in good agreement with the measured points as shown in Fig. 7 and Table 1. The $LaNi_{4.55}Al_{0.45}$ alloy has a smaller intrinsic degradation ratio R_{in} and poisoning rate constant k than $Mm_{0.9}Y_{0.1}Ni_{4.9}Mn_{0.1}$ alloy.

Under operating conditions of the refrigeration system, the air concentration in the alloy vessels is less than 0.2 vol.%. From calculation using this model, the degradation at 0.2 vol.% air after 200 cycles is only 10.4% in the $Mm_{0.9}Y_{0.1}Ni_{4.9}Mn_{0.1}$ alloy and 6.8% in the $LaNi_{4.55}Al_{0.45}$ alloy. Furthermore, the lost capacity, excluding the intrinsic capacity, is recovered by the reactivation process. Therefore, these alloys would be applicable to the refrigeration system with an appropriate reactivation process.

5. Conclusions

Air poisoning tests of the $Mm_{0.9}Y_{0.1}Ni_{4.9}Mn_{0.1}$ and $LaNi_{4.55}Al_{0.45}$ alloys led to the following conclusions.

- (1) The poisoned state is intermediate between the adsorption and the oxidation states.
- (2) Relations between the air concentration and the degradation rates are expressed by the proposed model derived from Langmuir's adsorption theory.

(3) The $\text{Mm}_{0.9}\text{Y}_{0.1}\text{Ni}_{4.9}\text{Mn}_{0.1}$ and $\text{LaNi}_{4.55}\text{Al}_{0.45}$ alloys have durability to air poisoning and are applicable to the refrigeration system.

References

- [1] I. Yonezu, K. Nasako, N. Honda and T. Sakai, *J. Less-Common Met.*, **89** (1983) 351.
- [2] K. Nasako, T. Yonesaki, I. Yonezu, S. Fujitani, T. Saito, M. Moroto, M. Osumi and N. Furukawa, *Proc. ISES Solar World Congress, 1989*, Vol. 2, Pergamon, Oxford, 1990, p. 1343.
- [3] M. Moroto, N. Hiro, K. Akashi, K. Nasako, T. Yonesaki and M. Osumi, The development of a refrigeration system using hydrogen absorbing alloys, *Sol. Eng. ASME*, (1991) 103.
- [4] K. Nasako, N. Hiro, K. Fukushima, M. Osumi, S. Fujitani and I. Yonezu, Solar refrigeration system using hydrogen-absorbing alloys, *Sol. Eng. ASME*, (1994) 373.
- [5] G.D. Sandroock and P.D. Goodell, *J. Less-Common Met.*, **73** (1980) 161.
- [6] F.G. Eisenberg and P.D. Goodell, *J. Less-Common Met.*, **89** (1983) 55.
- [7] P.D. Goodell, *J. Less-Common Met.*, **89** (1983) 45.
- [8] V.Z. Mordkovich, N.N. Korostyshysky, Yu.L. Baychtok, E. IZus, N.V. Dudakova and V.P. Mordovich, *Int. J. Hydrogen Energy*, **15** (10) (1990) 723.
- [9] F.R. Block and H.J. Bahs, *J. Less-Common Met.*, **89** (1983) 77.
- [10] S. Fujitani, H. Nakamura, A. Furukawa, K. Nasako, K. Satoh, T. Imoto, T. Saitoh and I. Yonezu, *Z. Phys. Chem.*, **179** (1993) 29.
- [11] T. Gamo, Y. Moriwaki, N. Yanagihara and T. Iwaki, *J. Less-Common Met.*, **89** (1983) 495.
- [12] G.D. Sandroock and P.D. Goodell, *J. Less-Common Met.*, **104** (1984) 159.
- [13] J.I. Han and J.Y. Lee, *J. Less-Common Met.*, **89** (1983) 45.